Brief communication: Alternation of thaw zones and deep permafrost in the cold climate conditions of the East Siberian Mountains, Suntar-Khayata Range

Robert Sysolyatin[1], Sergei Serikov[1], Anatoly Kirillin[1], Andrey Litovko[1] and Maxim Sivtsev[1]

[1]Melnikov Permafrost Institute, Yakutsk, 677000, Russia

Correspondence to: Robert Sysolyatin (robertseesaw@gmail.com)

Abstract. The Suntar-Khayata Range include numerous natural phenomena interacting or depending on permafrost conditions. Here, we examine some patterns of deep permafrost and talik zones on adjacent sites. A 210 m deep borehole in siltstone bedrock was equipped in July 2010 for temperature monitoring of the topmost 15 m and measurements of a deep permafrost temperature profile. The temperature curvature in the upper part has a bend which is consistent with at upper portion justify by climate warming and shows a steady-state linear geothermal profile below 85 m depth with a high geothermal heat flux. A shallow borehole situated at the river floodplain was used to investigate thaw zones temperature regime. Temperatures down to 6.7 m has been monitored at 5-min intervals during heavy rainfall and has had quite peculiar way. The thickness of the season freezing layer reach to 5.7 m, moreover ground temperature increases to 6 °C at 6.7 m depth by groundwater heat transfer. This study provides some new insight on the permafrost condition at one of the coldest places of Northern Hemisphere.

1 Introductions.

The East Siberian Mountains is one of the largest territory of east Siberia, but at the same time is researching how frontier permafrost region. On the other hand, the existing unique environmental conditions and natural cryosphere phenomena (glaciers, aufeis, "Pole of Cold" Oymyakon located at 63°15′N 143°9′E and Verkhoyansk located at 67°33′N 133°23′E e.g.) are interesting for the widespread scientific community (Lytkin and Galanin, 2016; Makarieva et al., 2022; Takahashi et al., 2011). Despite the increasing efforts in global permafrost mapping this area has almost no data on direct permafrost measurements and observations, which would be especially relevant in this data-scarce regions.

One of the main permafrost parameter is the permafrost thickness (Osterkamp and Gosink, 1991) which has considerably importance for paleo-climate reconstruction, hydrogeology description, deposit exploitation etc. The permafrost temperatures profile is controlled by initial surface temperature, bedrock thermal properties and geothermal heat flux (Lachenbruch and Marshall, 1986). Most frequently, the data about deep permafrost is acquired during geological-prospecting works for potential deposits. The expensive costs of deep borehole drilling limit its acquisition facilities, but in our case, we have access to a deep open borehole on gold ore deposit. In a previous study we focused on monitoring the active layer temperature regime by a widespread soil-pit network in an area close-by, but the temperature regime at the layer of zero annual amplitude (ZAA), season freezing layer as well as deep temperatures profiles have never been presented before (Sysolyatin et al., 2020).

For continuous permafrost of the East Siberia , taliks can exist under only specific condition because of having severe climate.~~In a cold climate with MAAT down to -12°C, taliks are almost certain to be avoided (Walvoord and Kurylyk, 2016).~~ Since the heat balance of the subarctic is clearly not cold enough to induce talik formation, groundwater

processes are more often involved. Taliks formed by thermal waters and open taliks (below large rivers) are well known, but taliks confined to coarse-grained permeable sediments of riverbanks are poorly studied (Makarieva et al., 2019). Floodplain sediments can accumulate water during the warm period and gradually empty in the winter (Mikhailov, 2015). The occurrence of such taliks forms a favorable environment for the growth thermophilic plants out of their species range – e.g., poplar, willow shrub formation.

In this brief communication, we present the thermal regime of typical permafrost and talik sites at the Suntar-Khayata Range. The successful embedding of a shallow borehole allows to examine the active layer temperature evolution in a floodplain talik for the first time. We aim to: 1) describe the typical permafrost conditions by possess data and discuss the present temperature changes 2) infer the possible extent of talik zones, discuss the origin of their formation and show the impact of heavy rainfall to ground temperature regime and slope stability. This study presents the general permafrost conditions and discusses possible ways to improve the permafrost mapping of the East Siberian Mountains.

2 Study area.

The Suntar-Khayata Range is located at the southern boundary of the East Siberian Mountains and serves as a watershed between Aldan and Indigirka River basins (Fig. 1). At altitudes between 2000 m asl and 2959 m asl a glacial area is persisting, representing largest of present glaciation in Siberia – with about 195 glaciers cover 163 km^2 (Ananicheva et al., 2010). The study area is represented by alpine relief with the height of the peaks from 1550 to 2031 m asl. The shallow borehole is located at the valley basin of Vostochnaya Khandyga River at 850 m asl (Fig. 1d), and the deep borehole is located in the narrow V-shaped valley Vostochnaya Khandyga tributary at 1100 m asl altitude (Fig. 1c). Late Paleozoic sandstone, siltstone and clay slate are prevalent bedrocks of the mountain rock, whereas the valley sediments consist of coarse-grained alluvium strata (Sokolov et al., 2015). Kurums exist at the foot and middle part of the mountain slopes and has widespread distribution (Lytkin and Galanin, 2016) and boulders can reach up to 3 m in diameter.

The climate conditions recorded at a weather station 43 km away from to east of the study site (Vostochnaya, WMO24679), situated at 1288 m asl. The MAAT ranges from -15.3°C to -11.2°C, average percipition is about 280 mm and maximum annual snow thickness vary from the 16 to 60 cm for the 1966-2018 period. Direct air temperature observation around the borehole at the floodplain shown the existence of winter temperature inversion at altitudes between 800 and 1400 m asl (Sysolyatin et al., 2020). The flora is not very diverse. Dwarf Siberian pine is occupying the top part of slopes between 1400 and 1600 m asl and able to accumulate significant snow cover. Siberian larch is growing on gentle and steep slopes, flat surfaces reflecting the most severe permafrost conditions. The poplars have a limited extent, adjacent to the riverbank.

According to our soil-pit monitoring network (Sysolyatin et al., 2020), the mean annual ground temperature ranges from -1.1 to -10.6°C at 1 m depth, active layer vary from 0.5 to 2.7 m and mean ground surface temperature can drop to -31°C. No direct observation of precipitation or snow thickness are available for the study area, but its influence is obviously significant. For instance, in 2021 anomalous heavy rains gave rise to numerous debris flows and the appearance of debris avalanches as well as an abrupt change in the talik temperature regime (Supplementary material, Fig. 3).

3 Materials and method

The deep borehole was drilled for prospecting of the orogenic gold deposit prospecting by a geological company in 1991. Organic material is almost absent and soil thickness does not exceed 0.5-0.8 m. Core samples (with marked

depths interval) were stocked close to the drilling site, where 4 samples have been collected for laboratory studies. In 2010 the sintered ice plug in the topmost 5 m was redrilled for establishing a temperature monitoring site. In 2020, temperature measurements were made at intervals of 5 m for depths of 20 to 150 m and 10 m for depths between 150 and 210 m using a movable high-precision negative temperature coefficient thermistor and multiconductor cable. To reduce the impact of convection, the hole was plugged by dense material.

The shallow borehole was drilled using a ~~wheeled~~ hummer drilling rig with air circulation in gravel alluvium sediments ~~without core sampling~~. Temperature disturbance was assumed to be negligible after a few days. The hole was cased with a PVC pipe with inner diameter of 20 mm and the sensors were inserted at 1, 3, 5 and 6.7 m depths. The space around the casing was filled by sand and well cutting. The first attempt to drill a borehole in the floodplain was reaching to a depth of 12 m, but a failure of drilling tools halted the process. At end of July the stratum was relatively dry.

Ground temperatures were monitored continuously within the shallow and deep borehole down to 6.7 and 15 m for one and 9 years, respectively. Measurements were made every 4 h with TMC50-HD thermistors that were attached to four-channel Onset HOBO data loggers (U12-008 model). Air and ground surface temperatures (2 cm depth) were acquired for the shallow borehole site using a 2-channel data logger (U23-003). The operation design of the different logger systems situated at sites and in interior of the boreholes is shown in Table 1. Since the sensors installed in the deep borehole at 5 and 15 m, we report the mean annual ground temperature determine the offset of heat wave penetration from surface. In accordance with local climatic conditions and thermal properties of the bedrock, to account for an equal seasonal cycle, MAGT was calculated for the periods September-August and January-December for depths of 5 and 15 m, respectively. For the shallow boreholes, the data presented for the high-frequency logging period (every 5 min) from 31 July to 8 September are used trace the impact of heavy rain infiltration events on the subsurface thermal regime.

4 Result

4.1 Permafrost temperature evolution

At the V-valley site, only two of four sensors (5 and 15 m) have useful and reliable data for analysis (Fig 2a and b). The ground temperatures below 0°C were recorded for the whole monitoring period at 5 m depth. The observed average MAGT is -4.25 °C for both depths. The ground temperature evolution show a sinusoidal pattern with smooth drifting following the changing climate condition. At 5- and 15 m depth, the amplitude ranges from 6.2 to 0.6 °C, respectively, for the whole measurement period. The fluctuations of mean annual ground temperature did not exceed 0.61 °C at 5 m and 0.26 °C at 15 m. The warming trend that has been highlighted for the 2010 to 2015 period was changing to equivalent cooling until 2019 at both depths. In accordance with the results presented, the ZAA depth might vary from 10.9 to 13.9 for a thermal diffusivity of around $1.21\text{-}1.96\times10^{-6}$ m² s^{-1} by core samples. However, as far as the temperature altering should not up over to 0.1 °C by annual period, the ZAA layer has been exceed 15 m depth.

4.2 Permafrost thickness and thermal conditions

The permafrost thickness observed by these direct measurements does not exceed 205-210 m in the deep borehole at V-valley. A detailed temperature profile is presented in Fig. 2c. Below the assumed depth of ZAA (20 m), the permafrost temperature increases downwards with a gradient ranging from 0.01 to 0.038 °C$^-$ m. From the whole

114 temperature curve the mean gradient was calculated as 0.0214 °C⁻m. The initial surface temperature (T_0=-5.25 °C) is

115 obtained by best-fit linear extrapolation from a depth interval of 85-160 m due to the uniform value of the gradient

116 (Lachenbruch and Marshall, 1986). The values for the temperature anomaly (offset value from linear fit) at 20 m (A_{20})

117 and 40 m (A_{40}), were calculated as 0.70 and 0.39 °C, respectively.

4.3 Talik temperature regime

119 A simple geomorphology sketch of the shallow borehole site is present in Figure 3a and an annual and monthly

120 temperature-time series for the floodplain site are shown in Figure 3b and c, respectively. The pattern of the 1 m depth

121 temperature evolution is consistent with the air and surface temperature evolution. Temperatures ranged from -6.3 to

122 6.6 °C and from -13.7 to 20.7 °C, respectively. Surprisingly, the temperature variation at 3m depth has been smaller

123 than for the sensors below, just from -2 to 1.6 °C. Refreezing at 3 m depth began at the end of January and the zero-

124 curtain period is present from approximately the end of June to September, dividing the floodplain (overburden)

125 sediments into to 3 zones – upper active layer, intermediate frozen layer and bottom permanent talik. The spike in

126 Figure 3c is related to percolation of warm rainwater to 3 m depth, probably through casing tube. The most peculiar

127 temperature behavior is found for the 5 and 6.7 m depth sensors, which is surely related to heat advection of ground

128 water movement. Patterns of temperature changes at 5 m depth are more linear, whereas at 6.7 m it is more exponential.

129 The maximum absolute temperature ranged between 4.4 °C (5 m) and 7.7 °C (6.7 m), while minimum temperatures

130 oscillated between -0.2 °C (5 m) and 0.3 °C (6.7 m). The ground at a depth of 5 m remained unfrozen for more than

131 75% of the time of the year. In an isopleth plot the talik appears below to 5.7 m and obviously continuous downward

132 (Fig 3b). At an air temperature of -9.9 °C and MAGST of -1.8 °C the MAGT for the observation period (almost a

133 year) is -1.1, -0.1, 1.1, 1.8 °C for depths of 1, 3, 5 and 6.7 m, respectively.

5 Discussion

135 Permafrost thickness is one of the major components of the cryosphere and has a close relation to geothermal heat

136 flux. According to Balobaev et al. (1985) the Suntar-Khayat Range is characterised by high values of geothermal heat

137 flux up to 0.08-0.10 Wm⁻² usually concentrating under narrow V-shaped valleys. Through numerous geothermal

138 measurements at the next orogenic gold deposits (Nezjdaninskoye) specific patterns of thermal conditions were

139 determined. Thus, the angle of inclination of the surface reduces the geothermal heat flux according to the equation:

140 $$q = q_0 cos\alpha \tag{1}$$

141 where q – calculated geothermal heat flux; q_0 – initial geothermal heat flux, α – slope angle.

142 The interaction between altitude and surface temperature has also been presented in previous studies and might

143 decrease MAGST to -6.5°C at 1800 m asl mountain peaks (Sysolyatin et al., 2020). As mentioned above, MAGT at 5

144 m depth have rather similar value to the ZAA temperature. By the steady-state equation (2) and expect the decrease

145 of the ZAA temperature upon upward height, the permafrost thickness was calculated (Table 1) (Carslow and Jager,

146 1959; Guglielmin et al., 2011). By corn samples, bedrock effective thermal conductivity is 2.41 Wm⁻¹ K⁻¹ and q_0=

147 0.052 Wm⁻² in permafrost body at base altitude surface level – 1100 m According to the orographic configuration of

148 the study area, the permafrost thickness at local peaks 2000 m asl can reach to ~ 500 m.

149 $$Z = T * \frac{\lambda}{q} + ZAA \tag{2}$$

150 where, Z – estimated permafrost thickness, m; T – temperature at the ZAA depth, °C; λ – effective thermal

151 conductivity, Wm⁻¹ °C⁻¹; q – geothermal heat flux in permafrost Wm⁻² (from equation 1).

152 Extrapolation of the linear portion of temperature curve to the surface result in significant differences to the current

153 temperature curve from the initial MAGST features (Lachenbruch and Marshall, 1986). Two variants of changes are

154 considered, a temperature change at the surface and a temperature change at the ZAA. For instance, assuming thermal

155 diffusivity is 1.6×10^{-6} m² s ⁻¹, the surface temperature shift around 1.4 °C would be ongoing from 22 to 81-year respect

156 to step, linear or exponential way of changes. When the temperature shifts by 0.7°C at the ZAA, the response time

157 will expand to a range of 19 to 90 years. With the available data about the rate of air temperature change at the closest

158 weather station, the second variant is the most plausible. It should be noted that the snow cover can change the surface

159 temperature by more than 5 °C (Gisnas et al., 2014), which is much larger than the air temperature change over the

160 last 80 years (IPCC, 2014).

161 As mentioned above, the talik appearance can only be caused by the thermal influence of superficial or ground water

162 in the cold environments of northeastern Siberia. The absence of permafrost under large rivers and in the areas adjacent

163 to hot springs is well-known. Nevertheless, in our case, where the distance from the main stream exceeds 1 km, the

164 presence of the talik was not assumed before. The reason for the existence of the talik is ambiguous. One possibility

165 is the migration of rainwater infiltrating through the "windows" of the kurums (block streams) on the adjacent slope.

166 The timing of the thermal impact of rainfall is clearly evident on the temperature graph at a depth of 1 m. These spikes

167 have been well explained before (Hinkel et al., 2001). The divergent temperature response at depths of 5 and 6.7 m is

168 difficult to explain, perhaps it may be related to the interaction of rainfall with the permafrost occurrence at depth. It

169 could also have been due to a delay in the influence of groundwater supply from the river. However, the response time

170 is largely consistent with the first hypothesis. The influence of groundwater from the river when considering the

171 thawing cycle is certain. On the isopleth plot it is clearly shown that the temperature at the depth of 5 and 6.7 m begins

172 to increase earlier than at a depth of 3 m, which means the proximity to the groundwater is accelerating warming for

173 the coarse-grained sediments. To solve this issue, it would be necessary to install additional piezometric and

174 temperature monitoring sites, as well as to carry out temperature measurements of the river water.

175 The interactions between groundwater and permafrost have been examine in a numerous study (e.g. Ge et al., 2011;

176 Kane et al., 2013; Walvoord and Kurylyk, 2016). The But the features of floodplain taliks for Kolyma region are

177 considered rather recently and are not well understood (Mikhailov, 2015). It is noted as the crucial reason for the

178 formation of the winter river flow. Floodplain taliks of the region are capable to accumulate huge amounts of water

179 and gradually return it back to the river during low-flow cold season. The main influencing factors are the slope of

180 the river floodplain and the permeability of the sediments. The volume of sand backfill material usually reduce

181 downward to aquiclude that increase permeable and capaciousness of aquifer. Probably the reason for the appearance

182 of such a large talik is just related to the site-specific conditions of the study area. A sufficiently reliable marker may

183 be the areal of poplar trees, tending to warmer environments. However, in our case, at the drilling site the vegetation

184 was represented by mosses and larch that is more typical for permafrost landscapes.

185 An increase in liquid precipitation, along with increase in air temperature, is one of the most obvious consequences

186 of global warming (Savelieva et al., 2000; Yang et al., 2005). For the permafrost zone, heavy rainfall often acts as a

187 trigger for geomorphological processes (Borgatti and Soldati, 2013). The effect of heavy rainfalls on permafrost is

188 most pronounced for the mountainous areas.

189 The behavior of the upper part of the permafrost during flooding rains, creates reasons for the activation of slope
190 processes. Heavy rains at the end of August 2021 were the trigger for 7 large landslides on a 5 km section of the
191 Kolyma highway, temporarily stopping traffic (Supplementary material). The high concentration of landslides on this
192 section is explained by the aspect and angle of the slope, creating favorable conditions for an increase of the active
193 layer. Abrupt and abundant saturation with rainwater led to critical weighting of soil material, after which the stability
194 of the slope has been disrupted. Landslide processes were also observed everywhere during field investigations in
195 other areas with a lower inclination and northern and eastern aspects. Descriptions of such scenarios are given in many
196 sources, but the detailed process for regions of northeastern Siberia is poorly understood at this time (Frauenfelder et
197 al., 2018; Geertsema et al., 2006; Gruber and Haeberli, 2007).

198 **6 Conclusion**

199 This study provides insight into thermal patterns of permafrost and talik that can be valuable for future studies of the
200 East Siberian Mountains. Permafrost is almost continuously distributed with a thickness reach to 500 m. Thermal
201 properties of the bedrock were obtained through laboratory determinations and a negligible permafrost temperature
202 trend was identified as a result of long-term monitoring. Due to the successful location of the borehole and high-
203 frequency measurements during rare heavy rains in August 2021, unusually high values of daily precipitation were
204 recorded in the Suntar Khayata Mountains (Verkhoyansk Ridge, Siberia). Due to the abundance of liquid precipitation,
205 peculiarities of the configuration of permafrost and thaw zones, as well as site morphology, the temperature regime
206 of soils has a peculiar feature down to a depth of 6.7 m. The size of the talik zone can be very significant, which must
207 be taken into account in mapping, design and modeling. A wide range of multidisciplinary research is required to
208 improve the understanding of permafrost conditions in this area.

209 *Data availability*

210 The data are available from the authors upon request.

211 *Supplement*

212 Debris landslides evidence are added at Supplement material.

213 *Author contributions*

214 RG and SS proposed the initial idea and carried out this study by designing researching sites, analyzing data, and
215 organizing and was responsible for the compilation and quality control of the observations. RG, SS, AL and MS
216 handled with field works. AK responsible for laboratory determination of rock thermal properties. RG prepared the
217 manuscript with contributions from SS, AK, AL and MS.

218 *Competing interests*

219 The authors declare that they have no conflict of interest.

220 **Acknowledgments**

221 This study has been funded by Republic of Sakha (Yakutia) and Russian Science Foundation (project N 22-27-20073).
222 The authors acknowledge the Melnikov Permafrost Institute for logistic and field work support. Finally, we thank the
223 reviewer Lutz Schirrmeister, anonymous reviewer, and editor Christian Hauck for comments and suggestions which
224 helped improve the manuscript.

225 **References**

226 Ananicheva, M. D., Krenke, A. N. and Barry, R. G.: The Northeast Asia mountain glaciers in the near future by
227 AOGCM scenarios, Cryosph., 4(4), 435–445, doi:10.5194/tc-4-435-2010, 2010.

228 Balobaev, V. T., Devyatkin, V. N., Gavriliev, R. I. and Rusakov, V. G.: About geothermophysical researching of
229 mineral deposits at north-east region, Geol. Geol. Explor., 5, 36–37, 1985.

230 Borgatti, L. and Soldati, M.: 7.30 Hillslope Processes and Climate Change, in Treatise on Geomorphology, pp. 306–
231 319, Elsevier., 2013.

232 Carslow, H. S. and Jager, J. C.: Conduction of Heat in Solids, Oxford University Press: New York., 1959.

233 Frauenfelder, R., Isaksen, K., Lato, M. J. and Noetzli, J.: Ground thermal and geomechanical conditions in a
234 permafrost-affected high-latitude rock avalanche site (Polvartinden, northern Norway), Cryosph., 12(4), 1531–1550,
235 doi:10.5194/tc-12-1531-2018, 2018.

236 Ge, S., McKenzie, J., Voss, C. and Wu, Q.: Exchange of groundwater and surface-water mediated by permafrost
237 response to seasonal and long term air temperature variation, Geophys. Res. Lett., 38(14), L14402,
238 doi:10.1029/2011GL047911, 2011.

239 Geertsema, M., Clague, J. J., Schwab, J. W. and Evans, S. G.: An overview of recent large catastrophic landslides in
240 northern British Columbia, Canada, Eng. Geol., 83(1–3), 120–143, doi:10.1016/j.enggeo.2005.06.028, 2006.

241 Gisnas, K., Westermann, S., Schuler, T. V, Litherland, T., Isaksen, K., Boike, J. and Etzelmuller, B.: A statistical
242 approach to represent small-scale variability of permafrost temperatures due to snow cover, Cryosphere, 8(6), 2063–
243 2074, doi:10.5194/tc-8-2063-2014, 2014.

244 Gruber, S. and Haeberli, W.: Permafrost in steep bedrock slopes and its temperature-related destabilization
245 following climate change, J. Geophys. Res. Surf., 112(F2), doi:10.1029/2006jf000547, 2007.

246 Guglielmin, M., Balks, M. R., Adlam, L. S. and Baio, F.: Permafrost Thermal Regime from Two 30-m Deep
247 Boreholes in Southern Victoria Land, Antarctica, Permafr. Periglac. Process., 22(2), 129–139, doi:10.1002/ppp.715,
248 2011.

249 Hinkel, K. M., Paetzold, F., Nelson, F. E. and Bockheim, J. G.: Patterns of soil temperature and moisture in the
250 active layer and upper permafrost at Barrow, Alaska: 1993–1999, Glob. Planet. Change, 29(3–4), 293–309,
251 doi:10.1016/S0921-8181(01)00096-0, 2001.

252 IPCC: Climate Change 2014, in Synthesis Report, Contribution of Working Groups I, II and III to the Fifth
253 Assessment Report of the Intergovernmental Panel on Climate Change, p. 151, Geneva, Switzerland., 2014.

254 Kane, D. L., Yoshikawa, K. and McNamara, J. P.: Regional groundwater flow in an area mapped as continuous
255 permafrost, NE Alaska (USA), Hydrogeol. J., 21(1), 41–52, doi:10.1007/s10040-012-0937-0, 2013.

256 Lachenbruch, A. H. and Marshall, B. V.: Changing Climate: Geothermal Evidence from Permafrost in the Alaskan
257 Arctic, Science (80-.)., 234(4777), 689–696, doi:10.1126/science.234.4777.689, 1986.

258 Lytkin, V. M. and Galanin, A. A.: Rock glaciers in the Suntar-Khayata Range, Ice Snow, 56(4), 511–524,
259 doi:10.15356/2076-6734-2016-4-511-524, 2016.

260 Makarieva, O., Nesterova, N., Post, D. A., Sherstyukov, A. and Lebedeva, L.: Warming temperatures are impacting
261 the hydrometeorological regime of Russian rivers in the zone of continuous permafrost, Cryosph., 13(6), 1635–
262 1659, doi:10.5194/tc-13-1635-2019, 2019.

263 Makarieva, O., Nesterova, N., Shikhov, A., Zemlianskova, A., Luo, D., Ostashov, A. and Alexeev, V.: Giant
264 Aufeis—Unknown Glaciation in North-Eastern Eurasia According to Landsat Images 2013–2019, Remote Sens.,
265 14(17), 4248, doi:10.3390/rs14174248, 2022.

266 Mikhailov, V. M.: Geographical regularities of distribution of floodplain taliks, Izv. Ross. Akad. Nauk. Seriya
267 Geogr., (1), 65, doi:10.15356/0373-2444-2014-1-65-74, 2015.

268 Osterkamp, T. E. and Gosink, J. P.: Variations in permafrost thickness in response to changes in paleoclimate, J.
269 Geophys. Res. Solid Earth, 96(B3), 4423–4434, doi:10.1029/90JB02492, 1991.

270 Savelieva, N. ., Semiletov, I. ., Vasilevskaya, L. . and Pugach, S. .: A climate shift in seasonal values of
271 meteorological and hydrological parameters for Northeastern Asia, Prog. Oceanogr., 47(2–4), 279–297,
272 doi:10.1016/S0079-6611(00)00039-2, 2000.

273 Sokolov, S. D., Tuchkova, M. I., Ganelin, A. V., Bondarenko, G. E. and Layer, P.: Tectonics of the South Anyui
274 Suture, Northeastern Asia, Geotectonics, 49(1), 3–26, doi:10.1134/S0016852115010057, 2015.

275 Sysolyatin, R., Serikov, S., Zheleznyak, M., Tikhonravova, Y., Skachkov, Y., Zhizhin, V. and Rojina, M.:
276 Temperature monitoring from 2012 to 2019 in central part of Suntar-Khayat Ridge, Russia, J. Mt. Sci., 17(10),
277 2321–2338, doi:10.1007/s11629-020-6175-3, 2020.

278 Takahashi, S., Sugiura, K., Kameda, T., Enomoto, H., Kononov, Y., Ananicheva, M. D. and Kapustin, G.: Response
279 of glaciers in the Suntar–Khayata range, eastern Siberia, to climate change, Ann. Glaciol., 52(58), 185–192,
280 doi:10.3189/172756411797252086, 2011.

281 Walvoord, M. A. and Kurylyk, B. L.: Hydrologic Impacts of Thawing Permafrost-A Review, Vadose Zo. J., 15(6),
282 vzj2016.01.0010, doi:10.2136/vzj2016.01.0010, 2016.

283 Yang, D., Kane, D., Zhang, Z., Legates, D. and Goodison, B.: Bias corrections of long-term (1973-2004) daily
284 precipitation data over the northern regions, Geophys. Res. Lett., 32(19), n/a-n/a, doi:10.1029/2005GL024057,
285 2005.

286

287

288

289

290

291

292

293

294

295

296

297
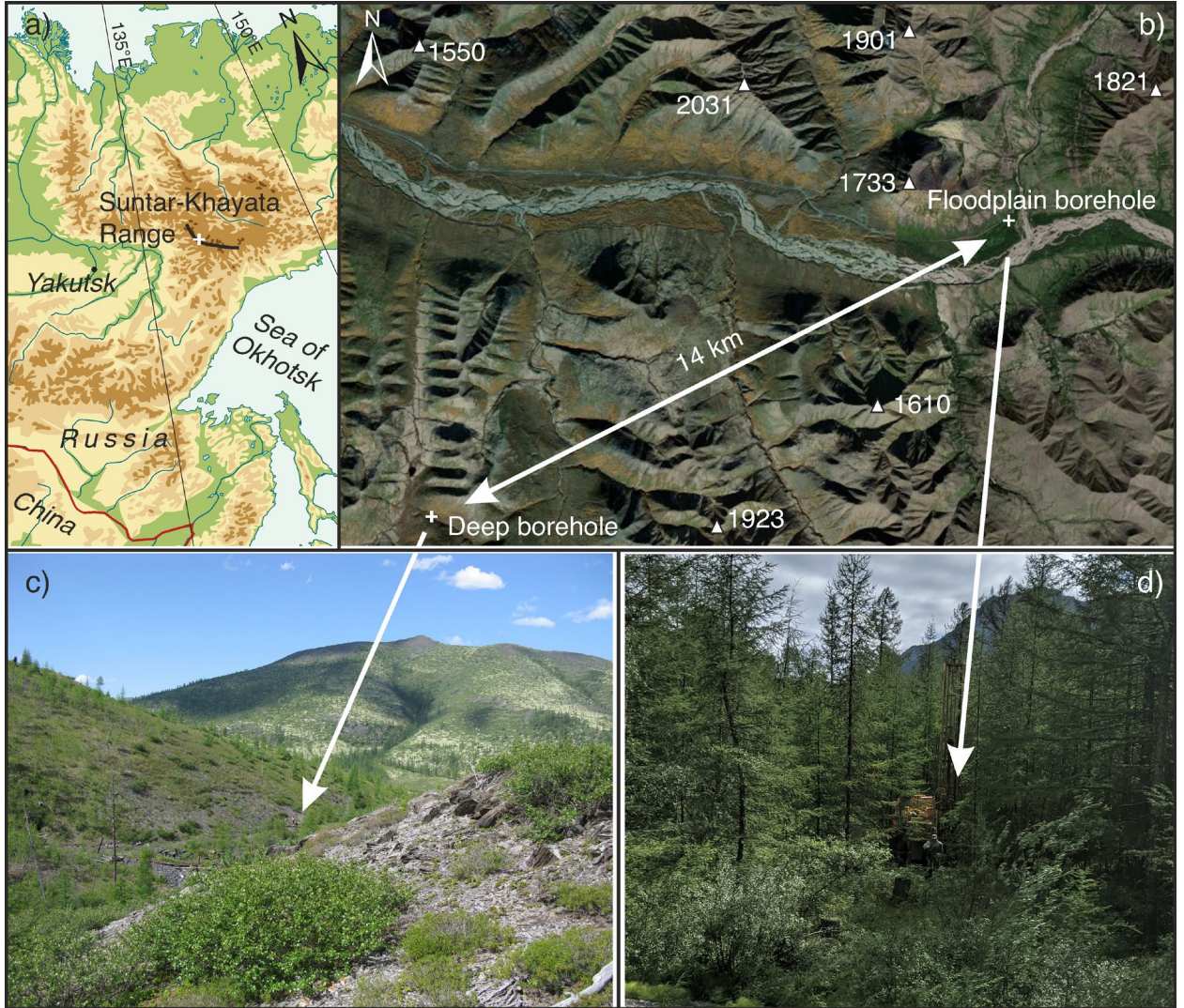
Figure 1. Study area description and picture of sites environment. In (a) a modified physical map of the location of the study area in eastern Siberia is shown (Map source: © GEOATLAS 1998). (b) MAXAR image of Vostochnaya Khandyga basin with altitudes of peaks. (c) Deep borehole site at V-shaping valley. (d) Shallow borehole site at river plain.

302
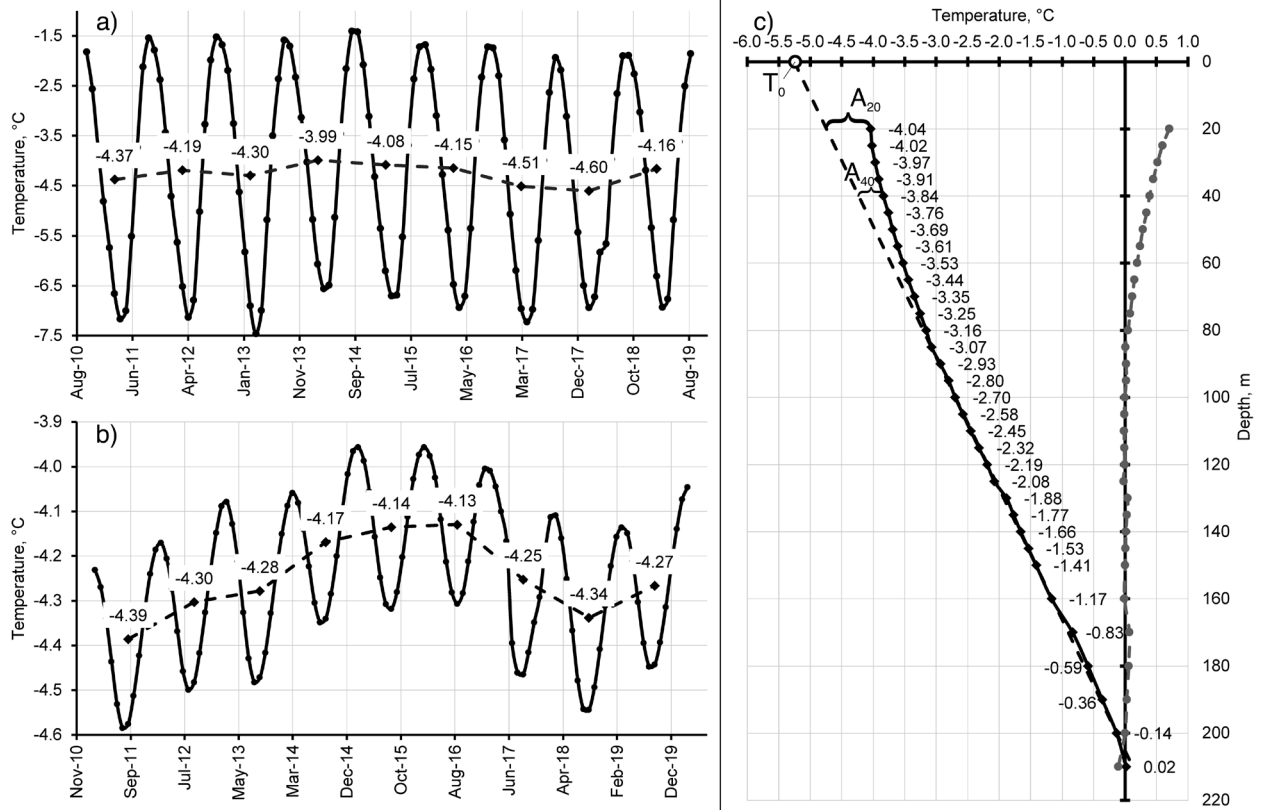
303

304 **Figure 2: Thermal regime of permafrost conditions in the deep borehole. Mean ~~mouthly~~monthly and annual ground**
305 **temperature evolution at 5 m (a) and 15 m (b) depth. (c) Temperature profile (solid line), best linear-fit (dashed line) and**
306 **current offset from extrapolated temperature (dotted line).**

307
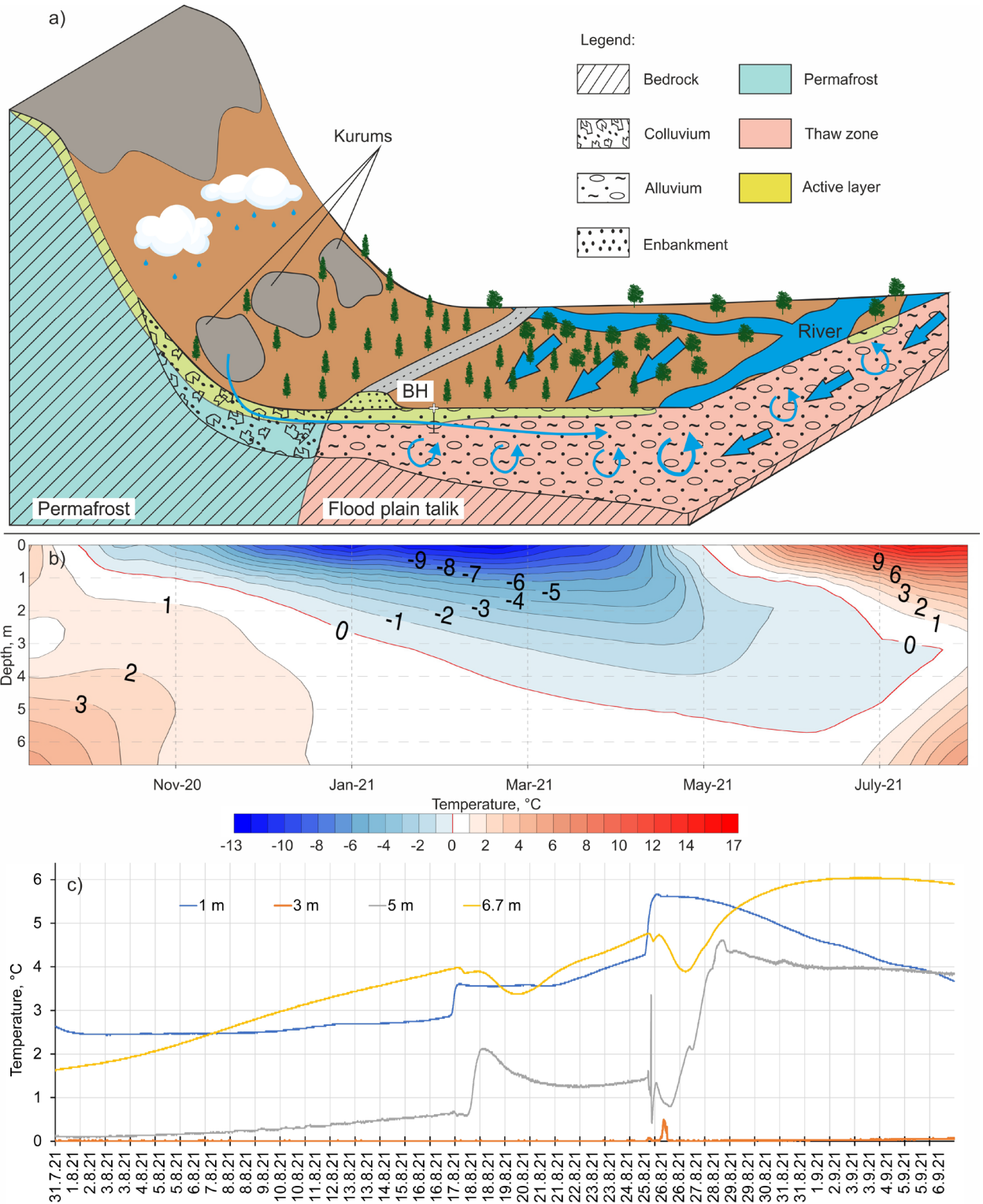
Figure 3: (a) The scenario of ground water flow of the floodplain talik. (b) Annual ground temperature evolution and (c) temperature fluctuation at a heavy rain event.

315

316 General parameters of equipment and operating timing of the loggers installed at different depths inside the
317 boreholes during the control period.

Location	Logger system and sensor	Accuracy and operation range	Sensor's depth, m	Measuring interval and operating time
River flood plain, Shallow borehole	OnSet Hobo U12-008	±0.25 °C at range -40 to 100 °C	1, 3, 5, 6.7	Every 5 min from 31-Jul-2021 to 7-Sep-2021/ Every 4 h from 8-Sep-2021 to 18-Aug-2022
River flood plain, Shallow borehole	OnSet Hobo U23-003		Air, Surface	
V-shaped valley, Deep borehole	OnSet Hobo U12-008		1*, 5, 10**, 15	Every 4 h from 20-Jul-2010 to 9-Sep-2021

318 *non valid cause to close position to borehole's iron case tube
319 **non valid because of misgiving temperature data at long period

320

321

322 Permafrost thickness based on the assumption that MAGT and permafrost heat flow are decreasing under step-up of
323 peaks height.

Peak altitude, m	Slope inclination (α), grad	Cos α	Temperature at ZAA (20 m depth), °C	q, Wm^{-2},	Permafrost thickness, m
1550	24.2	0.912	-5.5	0.047	298
1600	26.6	0.894	-5.7	0.047	314
1700	31.0	0.857	-6.0	0.045	343
1800	35.0	0.819	-6.5	0.043	386
1900	38.7	0.781	-7.0	0.041	434
2000	42.0	0.743	-7.5	0.039	486

324